Poly(glutaraldehyde)-Stabilized Fish Scale Fibrillar Collagen–Some Features of a New Material for Heavy Metal Sorption

Karine O. Moura, Eunice F. S. Vieira, Antonio R. Cestari

Laboratory of Materials and Calorimetry, Department of Chemistry/CCET, Sergipe Federal University, CEP 49100-000, São Cristóvão, Sergipe, Brazil

Received 11 February 2011; accepted 30 July 2011
DOI 10.1002/app.35398
Published online 4 November 2011 in Wiley Online Library (wileyonlinelibrary.com).

ABSTRACT: In this work, fibrillar collagen on scales of Corvina fish (Micropogonias furnieri) was crosslinked and used as a new adsorbent for sorption of Cr(VI) from aqueous solutions. Characterization has suggested that the crosslinked collagen of Corvina scale has higher denaturation temperature in relation to the raw scales. In addition, electrostatic interactions between collagen positive charges and chromate negative charges constitute the majority of the interactions. Solution microcalorimetry experiments have indicated that water swelling of the crosslinked scales is slightly exothermic and increased with increasing temperature. Sorption of Cr(VI) by crosslinked scales increases with increasing initial Cr(VI) concentration in solution and decreases with temperature increasing. The kinetic data of Cr(VI) sorption on crosslinked scales were best fitted to a multilinear exponential model. The values of Cr(VI) diffusion constants increase with both temperature and initial Cr(VI) concentration in solution. The maximum sorption capacity of the new adsorbent for Cr (VI) was found at 39 mg g^{-1} and is higher than some commercial adsorbent samples. So, chemically crosslinked Corvina scale is a promising adsorbent for sorption of Cr(VI) from aqueous solutions.
 J Appl Polym Sci 124: 3208–3221, 2012

Key words: Collagen; crosslinking; solution microcalorimetry; fish scales; Cr(VI) sorption

INTRODUCTION

Collagen is a polymer that exists as a triple helix with chains held together by hydrogen bonds. Several groups of collagen molecules have been classified based upon protein domain structures and macromolecular assemblies.[1] The most intriguing characteristic of collagen is the ability to self assemble into fibrils, providing the mechanical resilience and toughness needed for its adhesion properties. The chemical stability of collagens can be enhanced by crosslinking the molecule by physical or chemical means. Crosslinking agents and methods include aldehydes, carbodiimides, epoxides, diisocyanates, nonenzymatic glycosylation, dehydrothermal treatment, and ultraviolet light.[2] In general, glutaraldehyde (GA) is the most successful chemical agent and has received widespread acceptance. However, it was shown that polyglutaraldehyde is superior to glutaraldehyde as a protein crosslinking agent.[2] In reactions with proteins, polyglutaraldehyde gives rise to Michael addition or Schiff's base reactions which are stable and irreversible.

It is known that the presence of inorganic minerals improves the mechanical properties of collagens.[3] In this way, fish scales are composed of type I fibrillar collagen, and hydroxyapatites [$Ca_{10}(PO_4)_6(OH)_2$ or $Ca_5(PO_4)_3OH$]. Beyond several functions, type I collagen acts as a template for the deposition of the mineral phase.[4] Taking into account their characteristics, fish scales have gained attention of researchers as an alternative adsorbent to remove pollutants from aqueous solutions. The uptake abilities of scales are due to the presence of significant amounts of specific chemical groups of fish scales collagen, such as hydroxyl, carboxyl, amine and amide that are involved in the biosorption of heavy metals.[5] However, as far as we know, the synthesis and use of crosslinked fibrillar collagen on fish scales have not been reported in literature.

Chromium is a common pollutant introduced into natural waters due to the discharge of a variety of industrial wastewaters. According to the World Health Organization (WHO) drinking water guidelines, the maximum allowable limit for total chromium is 0.05 mg L^{-1}.[6] Species of Cr(VI) is mobile in the environment and is highly toxic and can easily penetrate the cell wall and exert its noxious influence in the cell itself, being also a source of various

Correspondence to: A. R. Cestari (cestari@ufs.br).
Contract grant sponsor: Brazilian agencies CAPES and CNPq.

cancer diseases.[7] At short-term exposure levels above the maximum contaminant level, Cr(VI) causes skin and stomach irritation or ulceration. Long-term exposure at levels above maximum contaminant can cause dermatitis, damage to liver, kidney circulation, nerve tissue damage, and death in large doses.[7]

Several methods have been reported for Cr(VI) removal such as reduction, filtration, reverse osmosis, ion-exchange, foam flotation, and electrolysis. These techniques present high selectivity and high efficiencies. However, they are not cost-effective, require tight operations and maintenance, and feed concentration must be monitored closely.[7,8] On the other hand, adsorption offers significant advantages like low cost, availability, profitability, easy of operation and efficiency, in comparison with conventional methods, especially from economical and environmental points of view. Biosorption of Cr(VI) from aqueous solutions is relatively a new process that has proven very promising in the removal of contaminants from aqueous effluents. Metal biosorption is a rather complex process affected by several factors. Adsorbent materials derived from low-cost agricultural and sea food wastes can be used for the effective removal and recovery of chromium ions from wastewater streams. The major advantages of biosorption over conventional treatment methods include: low cost, high efficiency, minimization of chemical and/or biological sludge regeneration of biosorbent, no additional nutrient requirement, and the possibility of metal recovery.[9]

A novelty of the work presented herein is the use of solution calorimetry to provide the hydrodynamic characterization of chemically crosslinked collagen on fish scale. Solution calorimetry is a technique that can be used to provide a way to determine energies of physical or chemical processes and may be of specific advantage in the study of specific processes occurring at polymer/solution interfaces systems without the need for additional analytical investigation.[10–12] This calorimetric technique permits the simultaneous determination of both the quantity and the energy of reaction. The experimental yield can potentially give information on thermodynamics of the process, energetics and analysis. However, less attention has been paid to the direct microcalorimetric investigations of heavy metals interactions on polymeric biosorbents.

In this work, the interaction of Cr(VI) on poly(glutaraldehyde)-crosslinked fish scale fibrillar collagen was investigated. Swelling characterization of the modified collagen was studied by immersion microcalorimetry, which permits direct determination of both the sorption amounts and the energies of swelling.

EXPERIMENTAL PART

Materials

Water was used after double-distillation. All the chemicals/reagents used in these studies were of Analytical Reagent Grade. Aqueous solutions of Cr(VI) was prepared by dissolving $K_2Cr_2O_7$ (VETEC, São Paulo, Brazil) in pH 4.0 HAc/NaAc buffered solution (ionic strength of 1.0×10^{-4} mol L^{-1}).

Biosorbent preparation

The raw Corvina fish (*Micropogonias furnieri*) scales were collected from the Fishermen's Market located in Aracaju, state of Sergipe, Brazil. Mature fish scales were washed repeatedly with water to remove adhering dust and soluble impurities from their surfaces. To preserve the structural characteristics of the collagen layer on the scales, the fish scale collagen was crosslinked under mild conditions using 0.05% (w/v) pH 7.0 water glutaraldehyde solution as described earlier.[13] A yellow pale material was obtained (hereafter described as GA-scale for simplicity) and cut into small 5×5 mm^2 square membranes of 0.5 mm of thickness and conditioned in a dark air-free flask.

Characterization of the materials

Thermogravimetric analyses (TG and DTG) of the materials were made using masses of about 10 mg, under nitrogen atmosphere from 25 to 1000°C, in a SDT 2960 thermoanalyzer, from TA Instruments. Infrared spectral data for scales before and after Cr(VI) sorption were obtained on a Perkin Elmer 1600 series FTIR spectrophotometer and diffuse reflectance accessory at a resolution of 4.0 cm^{-1}. The morphological characterization of the scales was carried out with a scanning electron microscope (SEM, JEOL-JSM 6360-LV). The samples were coated with gold (thickness of about 12 nm), and then SEM micrographs were obtained. The Raman spectra were acquired with a Bruker Senterra Raman System equipped with an Olympus microscope with a 50× objective to focus a Melles Griot laser beam on the sample. The spectra were excited by the 785 nm line from an air-cooled He–Ne laser. The laser power measured after the microscope objective was ca. 50 mW.

Determination of pHpzc of crosslinked scales

The determination of the pHpzc of the samples was carried out using a procedure similar as described earlier.[14] Briefly, 50 mL of 0.01 mol L^{-1} NaCl solutions were placed in closed Erlenmeyer flasks. The pH of each solution in each flask was adjusted to values of 2, 4, 6, 8, 10, and 12 by adding HCl

0.1 mol L^{-1} or NaOH 0.1 mol L^{-1} solutions. Then, 0.10 g of GA-scale was added and the final pH measured after 24 h under agitation at room temperature. The value of pHpzc of the scales of Corvina fish is determined from the points where the initial pH equals the final pH ($\Delta pH = 0$).

Microcalorimetry measurements

Microcalorimetric determinations were performed in a C80 microcalorimeter (SETARAM). Experimental determinations were performed using the membrane breaking (thin Teflon®) technique, as described elsewhere.[15] Briefly, 100 mg of GA-scale and 3.0 mL of water were put into the lower and the upper part of the calorimetric vessel, respectively. Calorimetric output is of thermal power (dq/dt; mW) as a function of time (t; s). The thermal effect of thin Teflon® membrane breaking for the empty cell was found to be negligible. The calorimetric experiments were carried out from 25 to 55°C (baseline precision of $\pm$ 10^{-4} mW). Each experiment was performed *in triplicate runs* and values are the average of them. The thermal effects and the corresponding swelling degree (SD) of GA-scale were simultaneously determined.[16] The SD values were determined according to the following formula: SD(%) = 100×[(wet fish scale mass − dried fish scale mass)]/(dried fish scale mass).

Kinetics of Cr(VI) sorption on crosslinked scales

Acetic acid/sodium acetate buffer solutions at pH 4.0 were used as solvent, because the sorption of Cr(VI) is maximized at this pH value.[17] The sorption kinetic experiments were performed by batch procedures, from 25 to 55°C (precision of 0.5°C), using Cr(VI) aqueous solutions at 0.05, 0.5, and 5.0×10^{-3} mol L^{-1}. These initial Cr(VI) concentrations values were chosen to verify the performance of the scales to remove low amounts of Cr(VI). In each sorption experiment, 50 mL of the Cr(VI) solution was added to 100 mg of GA-scale in a 150 mL polyethylene flask, and stirred continuously at a determined temperature, as described above. At predetermined times, samples were taken and the Cr(VI) concentration was determined by the diphenylcarbazide spectrophotometric method [17] at 540 nm wavelength (detection level less than 1.0 mg L^{-1}). The amount of Cr(VI) sorbed was calculated by using the following eq. (1):[18]

$$q_t = \frac{(C_i - C_t).V}{m} \quad (1)$$

where q_t is the fixed quantity of Cr(VI) per gram of fish scales after a given contact time t, in mol g^{-1}, C_i is the initial concentration of Cr(VI) in mol L^{-1}, C_t is the concentration of Cr(VI) present after a given contact time t, in mol L^{-1}, V is the volume of the solution in L, and m is the mass of fish scales in g.

RESULTS AND DISCUSSION

General considerations of chemical composition of fish scales and glutaraldehyde-crosslinked collagen

Fish scales are composed of an extracellular matrix, mainly type I fibrillar collagen, and hydroxyapatites [$Ca_{10}(PO_4)_6(OH)_2$ and/or $Ca_5(PO_4)_3OH$]. They present an average composition of 49.7% inorganic fraction and 50.3% of organic fraction.[19] Mineralization of fish scales occurs at the nucleation sites located in the extracellular matrix. Needle-shaped crystals of apatites can be found in the osseous layer and in fibrillary plates. The crystallographic long axes of apatites are preferentially parallel to the collagen fibres, also consistent with observations of collagen fibers and crystals of hydroxyapatite in bones. The polymeric structure of fibrillar collagen is composed of polypeptide chains with a triple-helical structure, and they are aggregated through hydrogen bonds to form collagen fibers.[19] However, collagens are soluble in both saline and acidic solutions. To overcome this undesirable characteristic, crosslinking reactions have been used for efficient insolubilization of collagen structure.[2]

Glutaraldehyde possesses unique characteristics that render it one of the most effective crosslinking reagents. It can be present in at least 10 different forms depending on solution conditions such as pH, concentration, temperature, etc.[20] Studies of collagen crosslinking reactions with monoaldehyde and dialdehydes having chain lengths of two to six carbon atoms demonstrated that the reactivity in this series is maximized at five carbons; thus glutaraldehyde is the most effective crosslinking agent.[20] Glutaraldehyde can react with several functional groups of proteins, such as amine, thiol, phenol, and imidazole because the most reactive amino acid side-chains are nucleophiles. Typically, reactions of glutaraldehyde with amines occur by aldol condensation or Michael-type addition, as shown in Figure 1. The linkage formed by the reaction of glutaraldehyde with an amino group has shown exceptional stability at extreme pH's and temperatures.[2,3] Despite the success of this reagent, its chemistry has been quite controversial.

In fact, glutaraldehyde structure in aqueous solution is not limited to the monomeric form. Commercial solutions are usually polymeric and contained significant amounts of α,β-unsaturated aldehydes that are able to form rings by loss of water molecules by aldol condensation. In fact, water is the medium in which commercial glutaraldehyde is

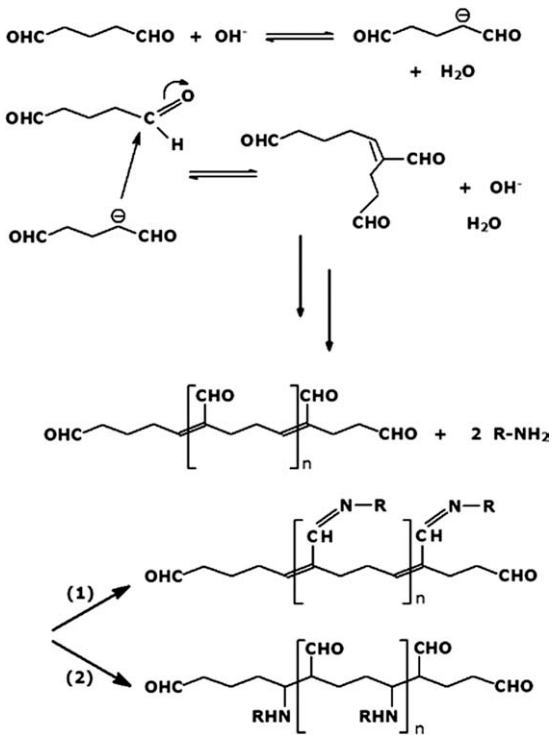

Figure 1 Esquematic representation of Schiff base (1) and Michael-type (2) reactions of (poly)glutaraldehyde with amine.

supplied and in which the crosslinking reaction with proteins is carried out, and glutaraldehyde was found to react with this solvent in various ways.[20] Upon dilution, the polymerized glutaraldehyde slowly converted to monomers, thus inducing a great variation in the relative abundances of monomeric and polymeric species in solution.

The chemical nature of the reaction of glutaraldehyde with proteins is not clearly understood, and the mechanisms of protein crosslinking reactions remain open to speculation. However, it seems that no single mechanism is responsible for glutaraldehyde reaction with proteins. In fact, because glutaraldehyde is present in different forms even for specific and controlled reaction conditions, several of the possible reaction mechanisms could proceed simultaneously.[20]

In general, the crosslinking of proteins generally implies the ε-amino group of lysine residues. The unprotonated amino groups are very reactive as nucleophilic agents. It should be noted that lysine ε-amino groups have pKa >9.5, but it is presumed that the small percentage of amines present in their unprotonated form at lower pH is sufficient to react with glutaraldehyde, which then drives the acid-base equilibrium to deprotonation of these groups for further reaction.[21] Most proteins contain many lysine residues, usually located on the protein surface (i.e., exposed to the aqueous medium) because of the polarity of the amine group. Some authors postulated pathways involving the reaction of the protein amino group with α,β-unsaturated aldehydes formed by aldol condensation of glutaraldehyde or reactions involving the conjugate addition of protein amino groups to ethylenic double bonds (Michael-type addition) of the α,β-unsaturated oligomers found in the commercial aqueous solutions of glutaraldehyde.[21] Monomeric glutaraldehyde can also be the active species involved in the crosslinking with proteins and the facility of polymeric forms to revert to the active monomer depended upon pH (i.e., the type of glutaraldehyde polymers in solution). However, polymers existing in the alkaline pH range cannot revert to the monomer because time and temperature tend to favor a more irreversible polymer, in contrast to polymers that exist at acidic and neutral pH.[20,21]

Characterization of the materials

Basic information on the structure is necessary for developing the use of GA-scale as adsorbent. Figure 2 shows the FTIR spectra of GA-scale before and after Cr(VI) interaction. The spectrum of raw scales was typical with O–H and N–H stretching band at 3257 cm^{-1}, NH–CO band at 1633 cm^{-1} and the methyl bending band at 1448 cm^{-1}. The spectra recorded absorption bands of P—O due to PO_4^{3-} groups in the 1009, 675, and 664 cm^{-1} region, which are characteristic of the inorganic phase (mainly hydroxyapatite), as well as of the H–O band of sorbed water.[22,23] The amide I band, with characteristic frequencies in the range from 1600 to 1700 cm^{-1}, was mainly associated with stretching vibrations of the carbonyl groups (C=O bond) along the polypeptide structure or the possible presence of some unreacted aldehyde groups in the scales. When comparing

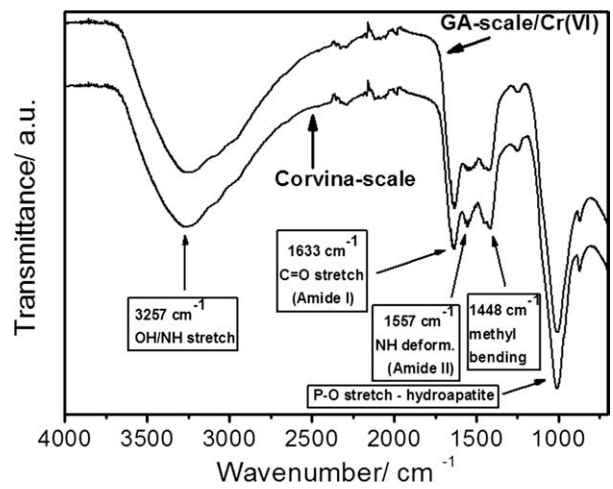

Figure 2 FTIR spectra of GA-scale before and after interaction with Cr(VI).

with the normal absorption range of the amide II bands position (1550–1600 cm^{-1}), the position is found to be shifted to lower frequency, 1557 cm^{-1}, which suggests the existence of hydrogen bonding in the collagen structure.[23]

Collagen fiber is low soluble in water but is a hydrophilic material. Water molecules are tightly bound to specific sites on collagen chains, or filling in the spaces between molecules ("interstitial waters").[24] These water molecules stabilize the triple helix structure of the collagen structure. From FTIR data, it is suggested that water molecules bind to the C=O and C—N polar groups of the collagen. For hydroxyapatite, during hydration processes, water was found to form strong electrostatic interactions with the calcium and the phosphate ions. This leads to several hydration layers exhibiting a strongly ordered character. Within these layers water mobility is reduced drastically.[24]

The uptake abilities of scales from different fish species should be similar because most fish scales contain significant portions of organic protein (collagen), and the analysis of the structure of collagen shows that it contains the possible functional groups, such as hydroxyl, carboxyl, amine and amides, that can be involved in interactions at fish scale/heavy metal interface. The FTIR spectrum of GA-scale with Cr(VI) sorbed is more or less the same in relation to the raw GA-scale. After Cr(VI) sorption, the relative intensity of the amide II spectral peak (1557 cm^{-1}) slightly decreased in intensity. According to literature data, shifts in FTIR spectra are not observed when heavy metals are sorbed on collagens.[25–27] It has only been observed partial disappearance of —NH stretching and –NH bending bands, which are related to the involvement of amino group of the collagen structure in biosorption process. In this way, after Cr(VI) sorption, the relative intensity of the amide II spectral peak (1557 cm^{-1}) slightly decreased in intensity. It is an indication that hydrophobic groups of the amide II of collagen structure seem to be a potential interaction site for Cr(VI) sorption on GA-scale. The mineral phosphate spectral region (900–1200 cm^{-1}) seems not to be affected.[25] So, it is more likely that the main Cr(VI) sorption sites are located on GA-scale. At low pH values, positively charged surface sites are formed, resulting in an overall positive surface charge. This is likely to assist in the attraction of negatively charged chromate ions to GA-scale functional groups through electrostatic forces. So, electrostatic interactions between GA-scale positive charges and chromate negative charges seem to constitute the majority of the interactions.[9,26,27]

Figure 3 shows the Raman spectra of the scales, before and after GA crosslinking. The most prominent peaks were found in the range of Raman shift

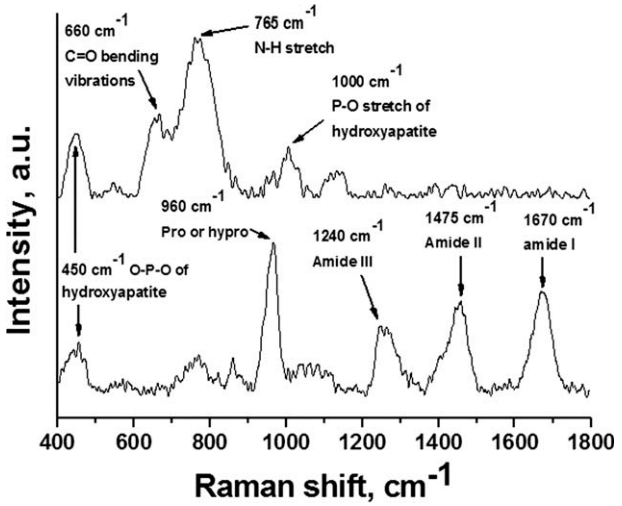

Figure 3 Raman spectra of Corvina scale before (lower part) and after (upper part) glutaraldehyde reaction.

from 400 to 1800 cm^{-1}. For the raw fish scale, the strong Raman band, centered around 1670 cm^{-1}, has been assigned to the amide I vibrational mode, which involves mainly C=O stretching vibrations, and partly, C—N stretching, C—C—N bending, and N—H in—plane bending of peptide groups or vibration of the thioester forms due to the presence of R—O—S—C— groups.[28] The amide II vibration around 1475 cm^{-1}, involves mainly N—H in-plane bending and C—N stretching of trans peptide groups. The amide III mode involves C—N stretching and N—H in plane bending vibrations of peptides. This Raman band is located in the 1200–1300 cm^{-1} range. The intensity of the amide III band for α-helix structure appears centered around 1240 cm^{-1}. Stretching vibrations of C—C appear in the 960–1000 cm^{-1} range, which are characteristic of α-helices. Proline and hydroxyproline (hypro) are amino acids of the connective tissue proteins such as collagen and hypro is landmark amino acid for collagen. Bands for proline and another for hypro residues appear around 800 cm^{-1} to 970 cm^{-1} and a peak centered around 960 cm^{-1} appeared in the spectrum of fish scale.[28]

Chemical modification might cause some effect on some amino acids of collagen. After reaction with GA, it was observed the absence of the peak at 960 cm^{-1}, suggesting reaction of GA with proline and hypro. The absorption band at around 765 cm^{-1} is relative to the N–H stretching, which is primarily due to the formation of imines, after reaction of collagen with GA. One other band centered around at 660 cm^{-1} has been assigned to C=O out-of plane bending vibrations. The peaks that appeared centered around 450 cm^{-1} are attributed to the symmetric O—P—O bending mode of hydroxyapatite of the fish scales.[28,29] The Raman spectrum of GA-scale

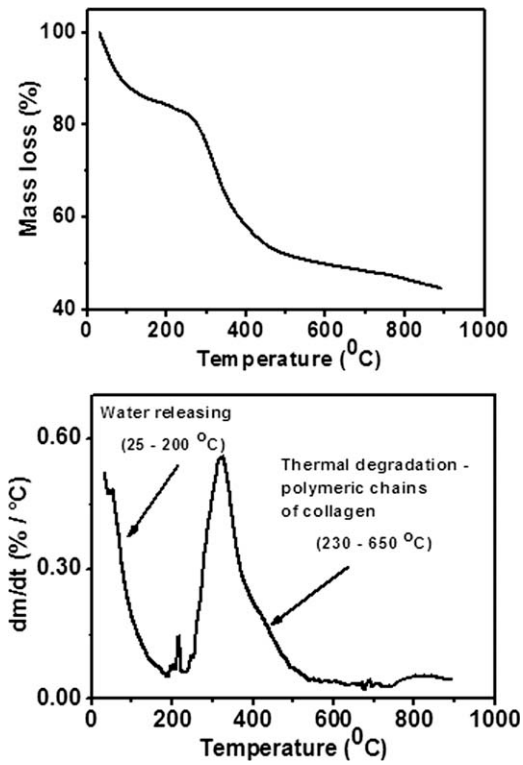

Figure 4 TG (upper part) and DTG (lower part) curves of GA-scale.

with Cr(VI) sorbed (not shown) is also very similar to the raw GA-scale, suggesting that attraction of negatively charged chromate ions to GA-scale functional groups through electrostatic forces. This is in agreement with the results obtained from FTIR spectroscopy.

TG-DTG plots of Corvina scales are shown in Figure 4. The scales are mostly composed of different organic matters, water and some amount of minerals. On heating GA-scale, two main weight loss events are shown at the following temperature ranges: 25–230, 250–630°C. In the DTG curve, two main peaks can be observed. The first event has been related to the superficial water releasing. The second event corresponds to the thermal degradation of the polymeric chains of collagen followed by the carbon material elimination. No differences of the thermal behavior of raw Corvina scale and GA-scale were clearly observed. Similar results are described in literature concerning thermal analysis of fish scales.[2,26]

Figure 5 displays the DTA curves of the scales, before and after glutaraldehyde crosslinking. The curve of the uncrosslinked scale exhibits an initial peak centered at about 32°C, associated to the denaturation temperature (T_d) of the fish scale collagen. However, it is observed the shift of T_d to a higher value (about 55°C) after GA crosslinking. The increased thermal stability exhibited by fish scale collagen has been ascribed to the presence of covalent bonds formed by the crosslinking reaction.[30]

Some features of GA-scale can be seen in the SEM micrographs (Fig. 6). It is possible to note two regions, one being white and the other being darker. The white region is rich in inorganic material containing high proportions of calcium and phosphorus (average Ca/P, atom,% = 1.69), whereas the dark region is rich in proteins.[21] The Ca/P ratio can be considered very close to the theoretical one described in literature for apatite structures (1.67).[30] Sheet-like structures composed of vertically oriented collagen fibers are also observed. Several fractures are also detectable along the radial discontinuity lines, probably as a consequence of crosslinking reaction or air-drying. Figure 6(c) has shown the presence of random-ordered calcification of needle-like or flaky crystals of apatites.

The X-ray diffractogram of a sample of GA-scale is shown in Figure 7. The broad peaks corresponding to the apatite structure reveled that scales show relatively low crystallinity levels. The main peaks are found in 2θ =, 25.7, 27.5, 31.8, 39.4, 46.6, 49.3, and 52.9° with d spacings from 0.170 to 0.345 nm. The obtained results are comparable with biological apatite containing structures.[22,23] However, the peak at about 2θ = 27.5° has also been associated with the presence of collagen.[31]

The pH where the net total particle charge is zero is called the point of zero charge (PZC). The GA-scale displays a PZC at pH_{pzc} = 7.0. If the pH is above its PZC the adsorbent surface will have a net negative charge and predominantly exhibit an ability to exchange, while the adsorbent will mainly retain anions (electrostatically) if its pH is below its PZC. At very low pH values (usually less than 3.0) also protonated species compete strongly with metal ions

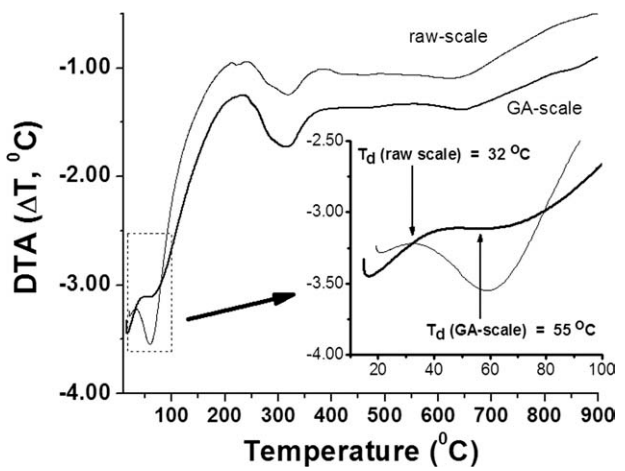

Figure 5 DTA curves of the scales before and after glutaraldehyde crosslinking. The insert shows the values of the temperature of denaturation (T_d) of the scales before and after glutaraldehyde crosslinking.

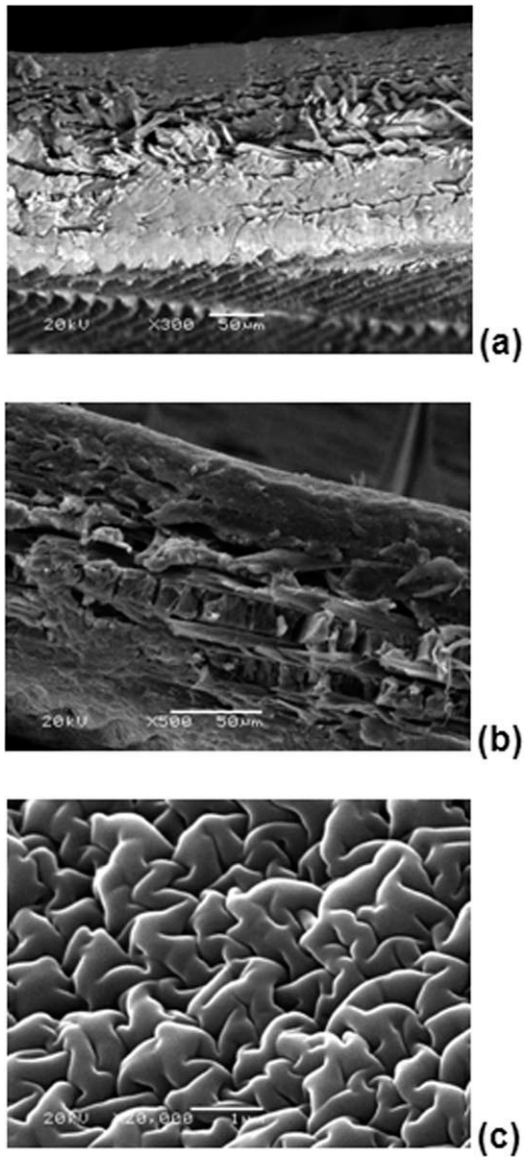

Figure 6 SEM micrographies of GA-scales. Magnifications of 300X (a), 500X (b), and 20,000X (c).

for the active sites, so sorption was small. When the pH was increased, electrostatic repulsion between cations and surface sites and the competing effect of hydrogen ions decreased and consequently the metal uptake was increased.[32]

Microcalorimetric analysis of water swelling of crosslinked scales

Hydrodynamic characterization under water swelling is important for practical uses of collagens. Collagen fiber is a hydrophilic material in nature. Water molecules are bound to specific sites on collagen chains, or filling in the spaces between molecules ("interstitial waters").[33] These water molecules stabilize the triple helix structure of the collagen structure. From FTIR data, it is suggested that water molecules bind to the C=O and C—N polar groups of the collagen. For hydroxyapatite, water interacts strongly with calcium and phosphate ions. This leads to several hydration layers exhibiting reduced water mobility.[34]

As most chemical and physical processes are accompanied by heat effects, isothermal solution calorimetry represents a unique technique to obtain direct information of both aspects, thermodynamics as well as kinetics. Microcalorimetric kinetic data are the foundation of mechanistic investigations, and many of the systems of interest at polymer/liquid interfaces are complex and present considerable difficulties in analysis. To obtain accurate kinetic parameters for fast processes from microcalorimetric outputs (up to about 40 min), it is necessary to apply Tian equation, to take into account the heat capacity and the rate of temperature change of the reaction vessel, as shown in eq. (2):[34]

$$S_{\mathrm{corr}}(t) = S_{\mathrm{orig}}(t) + \tau\left(\frac{dS_{\mathrm{orig}}(t)}{dt}\right) \tag{2}$$

where $S_{\mathrm{corr}}(t)$ is the corrected calorimetric signal (W), $S_{\mathrm{orig}}(t)$ is the original calorimetric signal (W), τ is the time constant of the calorimeter (150 s, in this work) and $[\mathrm{d}S_{\mathrm{orig}}(t)/\mathrm{d}t]$ is the time derivative of the original calorimetric signal.

It should also be known that the heat measured from flow calorimetry is an integral heat since there are different sites for water interaction in fish scales. The interaction enthalpy $\Delta_{\mathrm{int}}H$ can be calculated directly by the following eq. (3):[35]

$$-\Delta_{\mathrm{int}}H = \frac{Q_{\mathrm{int}}}{n_{\mathrm{int}}} \tag{3}$$

where, Q_{int} the integral interaction energy (J g^{-1}), n_{int} is the number of moles of the adsorbate (water in this work, mol g^{-1}).

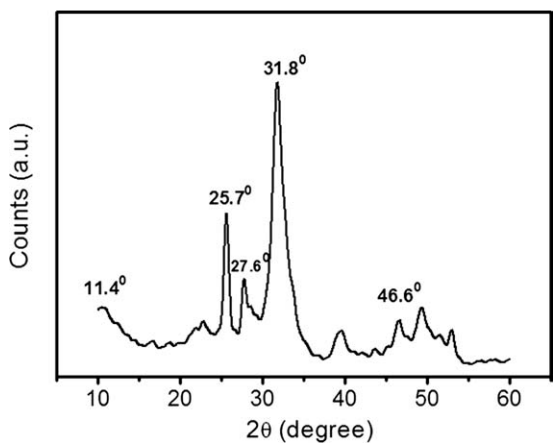

Figure 7 DRX diffractogram of GA-scale.

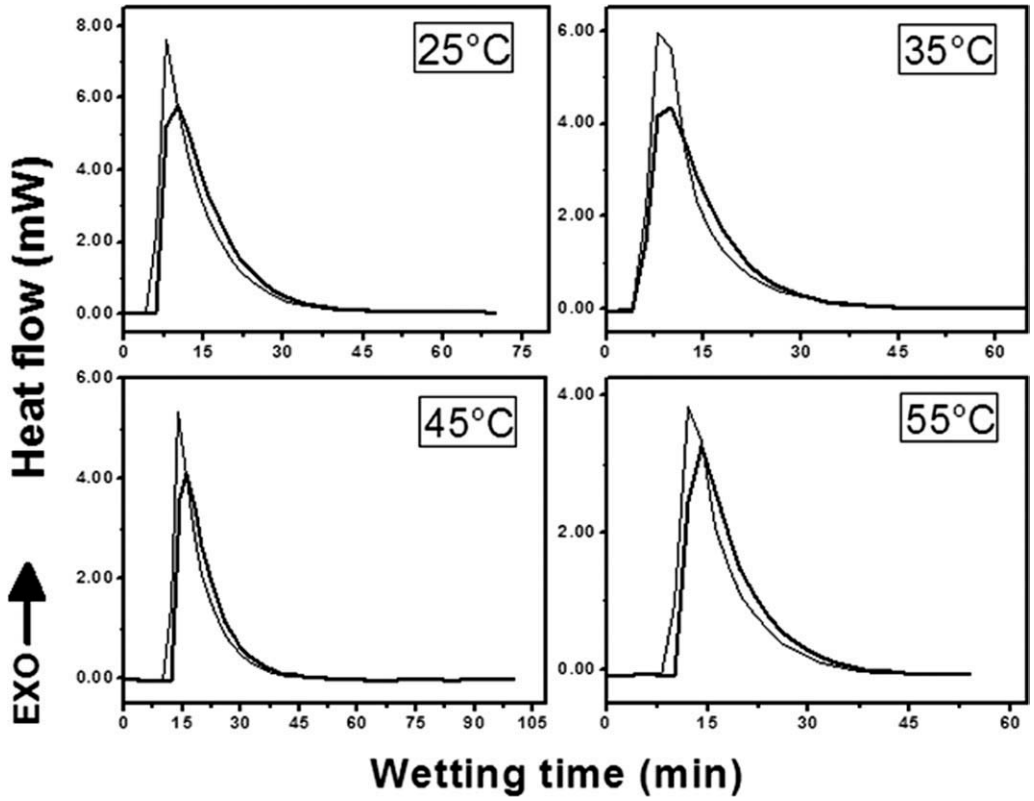

Figure 8 Microcalorimetric plots of the water swelling of GA-scales, at different temperatures. The thin curves are the uncorrected calorimetric output and thick curves are the calorimetric outputs after Tian equation correction.

The profiles of the microcalorimetric interaction processes are illustrated in Figure 8. The base line used for the integrations was selected as linear from first to last point, joining the two extreme points selected on the curves. The thermodynamic and kinetic parameters of the water swelling of GA-scale are presented in Table I. The values of SD of sorbed water decreased as temperature increases. The reaction time did not present significant changes in relation to temperature (from 40 to 45 min).

The enthalpies are slightly exothermic, and interaction energies decrease as temperature increases. In general, low exothermic interactions at polymer/liquid interfaces are in agreement with diffusion of fluidic phase (water) into internal interaction sites.[36] It has been suggested that the small magnitude of the sorption enthalpy is an average result of diffusional (endothermic) and chemical bonding (exothermic) processes.[37] Interactions at solid/liquid interfaces that occur with intense adsorbate diffusion present small and relatively similar values of $\Delta_{int}H$. Water transport through polymeric materials is generally described following an adsorption–diffusion mechanism, where molecules first diffuse from the bulk phase to the adsorbent surface. Next, they adsorb to the sites on the surface and diffuse through the adsorbent structure, driven by the chemical potential gradient within the pores.[34,36]

In this work, the swelling kinetic modeling was performed using isotherms built from the cumulative values of heat of swelling, which are presented in Figure 9. The cumulative calorimetric outputs are fitted to a simple exponential function shown in eq. (4):[38]

$$Q_{int} = Q^m_{int}(1 - \exp^{-(k.t)^n}) \quad (4)$$

Where Q_{int} and Q^m_{int} denote the energy release at a given time t and the maximum energy release of the swelling processes, respectively. The term k is the kinetic constant and n is another constant, which is related to the kinetic order.

TABLE I
Swelling Degree (SD), Thermodynamic (Q_{int} and $\Delta_{int}H$) and Kinetic (k and n) Parameters of the Water Swelling of Crosslinked Fibrillar Collagen on Corvina Scales in Relation to Temperature

Temperature (°C)	WA (%)[a]	$-Q_{int}$ (J g^{-1})[b]	$-\Delta_{int}H$ (kJ mol^{-1})[c]	k/10^{-2} (min^{-1})	n
25	45.3	40.18	1.58	6.04	2.29
35	39.0	31.20	1.52	6.58	2.32
45	37.8	26.30	1.29	5.67	3.87
55	30.8	20.30	0.95	5.32	4.05

[a] Average Standard Deviation (%) = 3.5.
[b] Average Standard Deviation (%) = 4.8.
[c] Average Standard Deviation (%) = 5.1.

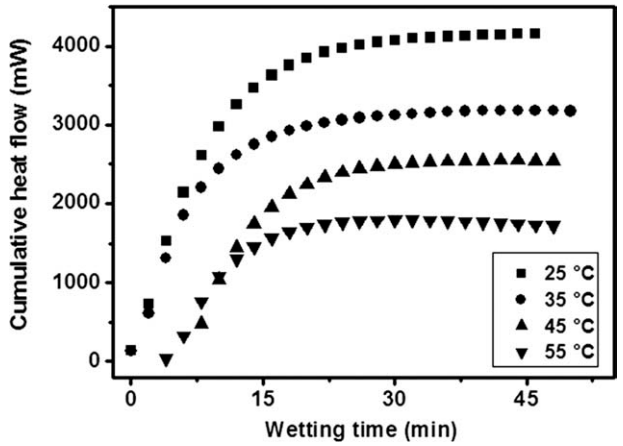

Figure 9 Typical profile of the cumulative heat flow curve of water swelling of GA-scale in relation to contact time.

Most often many different rate equations are tested in parallel and the appropriate best-fit procedures are used to verify whether one is better than another. The linear least-squares method (R^2), applied to the transformed kinetic data is usually adopted for this purpose.[39] However, R^2 is sensitive to extreme data points, resulting in misleading indication of the quality of fit. This is further complicated when the data points are subjected to linear transformations; existing extreme-points may disappear and new extreme-points may be created.[40] In this work, to evaluate the fitting of the exponential kinetic model, chi-square (χ^2) tests were done according to eq. (5):[41]

$$\chi^2 = \sum \frac{(Q_{\text{int},e} - Q_{\text{int},m})^2}{Q_{\text{int},m}} \quad (5)$$

where $Q_{\text{int},e}$ and $Q_{\text{int},m}$ are the energy release at a given time t, which were calculated using experimental data and the exponential kinetic model, respectively. The chi-square statistic test is basically the sum of the squares of the differences between the experimental data and theoretically predicted data from models. If modeled data are similar to the experimental data, χ^2 will be a small number; if they are different, χ^2 will be a large number.[41] Good agreements of the experimental and calculated data were found using the exponential model for all contact time evaluated (χ^2 less than 10.00). In general, the rate constants (k) decrease when temperature increases. However, the kinetic orders calculated (n) increase when temperature increases. This has been attributed, as can be noted from the swelling thermodynamic results found in this work, to the increase of water diffusion with temperature. So, internal diffusion of water seems to be the rate limiting step of the water swelling of the GA-scale.[42]

Modeling of sorption kinetics of Cr(VI) on crosslinked scales

In aqueous solutions, Cr(VI) anion is a series of chromate anions depending upon the pH of the solution. Between pH 2 and 6, $HCrO_4^-$ and $Cr_2O_7^{2-}$ are in equilibrium, the major specie is $HCrO_4^-$. As the pH increases, this form shifts to CrO_4^{2-} and $Cr_2O_7^{2-}$. At pH greater than 7.5, CrO_4^{2-} is the only chromate species in aqueous phase. When the pH value is less than 2, $HCrO_4^-$ and $Cr_2O_7^{2-}$ can transform $H_2Cr_2O_7$. With increase of pH, the degree of protonation of the surface of the adsorbent reduces gradually and hence sorption capacity decrease in the pH range of about 4.5–7. In addition, the lower affinity of Cr(VI) sorption above pH 7 has been attributed to the strong competition between HCrO4$^-$, $Cr_2O_7^{2-}$ and OH^- since more OH^- anions are present in solution.[9]

The curves of the sorption of Cr(VI) on GA-scale are presented in Figure 10. In general, sorption of Cr(VI) on GA-scale increased with contact time and temperature. The sorption equilibrium was established after about 300–400 min of contact time. The GA crosslinking did not change the values of Cr(VI) sorption on the fish scale significantly (average SD of the experimental values less than 3.0%). However, we have observed that the results obtained for adsorption of Cr (VI) using the crosslinked scales have presented better reproducibility (average SD of the experimental values less than 5.0%).

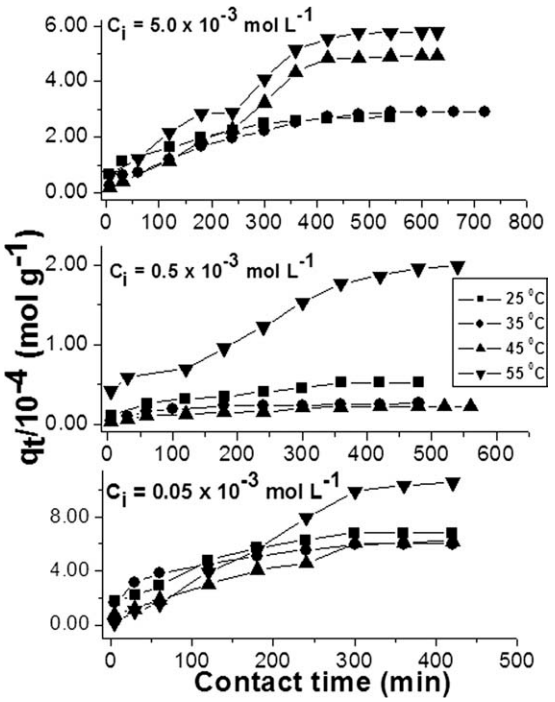

Figure 10 Cr(VI) sorption kinetics onto GA-scale in relation initial Cr(VI) concentration (C_i) and temperature. Symbols represent the experimental data and the solid lines through the data points are only to guide the eye.

It was found that the Cr(VI) sorption efficiency is 85–40 % when the initial Cr(VI) concentration in solution varied from 1.0×10^{-5} to 5.0×10^{-3} mol L^{-1} in 300 min of contact time. In addition, when the initial Cr(VI) in solution was very low (about 1.0 mg L^{-1}), the concentration of Cr(VI) in solution was observed to drop rapidly to less than 0.05 mg L^{-1} within 400 min. Thus, GA-scale can be considered a good adsorbent to remove Cr(VI). Higher adsorptions (in mol g^{-1}) were obtained when the initial concentration of Cr(VI) in solution is high, suggesting that this condition facilitates the access of Cr(VI) cations to the sorption sites. However, the percentage of retention may be low because the quantity of adsorbent sites is limited by the fixed adsorbent mass used in the sorption experiments.

The first major challenge for the adsorption field is to select the most promising types of adsorbent from an extremely large pool of readily available materials. The next real challenge is to identify the sorption mechanisms. Mechanisms involved in a biosorption process can include chemisorption, complexation, ion exchange and adsorption–complexation on surface. The sorption process can be described by the following consecutive steps (i) transport of solute in the bulk of the solution; (ii) diffusion of solute across the so-called liquid film surrounding sorbent particles; (iii) diffusion of solute in the liquid contained in the pores of sorbate particle and along the pore walls (intraparticle diffusion); (iv) adsorption and desorption of solute molecules on/from the sorbent surface. The overall sorption rate may mainly be controlled by any of these steps; a combined effect of a few steps is also possible.

In this work, we have used some traditional kinetic models for sorption systems at solid/liquid interfaces. Predicting the rate at which the pollutants removal takes place in a given solid/solution system is one of the most crucial factors for the effective sorption system design. Many attempts have been made to formulate general mathematical expressions, which would be able to adequately describe the kinetics of sorption in such systems. Their main advantage is simplicity and easiness when applying to correlate the data without necessity of using advanced computational procedures. The development of an appropriate model can be based on accepting a certain fundamental approach to interfacial kinetics and its further modification to adopt it for a given sorption system. This method has led to propose many expressions related to the concept of a chemical reaction occurring on the surface and its order. These include first-order and second-order irreversible reactions based on the solute concentrations.[43,44]

A simple kinetic analysis of sorption is the pseudo-first-order equation in the form:[43]

$$\frac{dq_t}{dt} = k_1(q_e - q_t) \tag{6}$$

where k_1 is the pseudo-first-order rate constant that relates to the amount of Cr(VI) sorbed by the scales and q_e denotes the amount of sorption at equilibrium. The linearized form of eq. (6) is:

$$\ln(q_e - q_t) = \ln(q_e) - k_1 t \tag{7}$$

In addition, a pseudo-second-order equation based on sorption equilibrium capacity may be expressed in the form:

$$\frac{dq_t}{dt} = k_2(q_e - q_t)^2 \tag{8}$$

where k_2 is the pseudo-second-order rate constant that relates to the amount of dye sorbed by the solid phase. The linearized form of eq. (8) is:

$$\frac{t}{q_t} = \frac{1}{k_2 q_e^2} + \frac{1}{q_e} t \tag{9}$$

The fitting validity of these models is traditionally checked by the linear plots of $\ln(q_e - q_t)$ vs. t, and (t/q_t) vs. t, respectively.[43,44] From the slope and intersection of the straight line obtained, the corresponding constant values for both models, for each temperature studied, provides the respective kinetic constants, k_i ($i = 1$ or 2), and the q_e parameters. In this work, the best linear fittings were detected using the pseudo-first-order kinetic model (χ^2 less than 5.29×10^{-4}).

However, for many sorption systems, the plots of either $\ln(q_e - q_t)$ against t and t/qt against t may be multilinear.[36] The kinetic parameters may vary with time, or the solid phase concentration (q_t) and the rate constants in the kinetic models may not be invariable. This leads to the idea of incorporating a q_t-dependent rate constant into the lumped kinetic models. In this way, an exponential kinetic equation was also used in this work. The Cr(VI) sorption should also be visualized using the Avrami exponential function, as shown in eq. (10):[16]

$$q_t = q_e(1 - \exp^{-[k_{av}t]^n}) \tag{10}$$

where k_{av} is the Avrami kinetic constant and n is another constant, which is related to the Cr(VI) sorption mechanism changes. The linearized form of this equation is presented in eq. (11):

$$\ln\left(\ln\left(\frac{q_e}{q_e - q_t}\right)\right) = n \ln k_{Av} + n \ln t \tag{11}$$

The slopes and intersections values of the $\ln(\ln(q_e/q_e\text{-}q_t))$ *vs* $\ln t$ plots provide the n and $ln\ k_{av}$ values,

TABLE II
Kinetic Parameters of the Pseudo-First- and Pseudo-Second-Kinetic Models for Sorption of Cr(VI) on Crosslinked Fibrillar Collagen on Corvina Scales

		Pseudo-first-order			Pseudo-second-order		
$C_i/10^{-4}$ (mol L^{-1})	Temperature (°C)	$\chi^2/10^{-4}$	$Q_e/10^{-5}$ (mol g^{-1})	$k_1/10^{-2}$ (min^{-1})	$\chi^2/10^{-7}$	$Q_e/10^{-5}$ (mol g^{-1})	$k_2/10^{-2}$ (g $mol^{-1}min^{-1}$)
0.10	25	0.01	0.09	1.80	2.87	0.08	199
	35	0.01	0.09	1.21	0.07	0.08	105
	45	0.05	0.18	1.56	1.18	0.14	14.1
	55	0.05	0.08	0.20	2.49	0.31	4.06
3.00	25	5.29	83.9	3.03	211	6.03	1.99
	35	1.32	1.47	0.81	10.7	2.73	9.68
	45	0.28	3.01	1.01	41.8	2.64	3.80
	55	0.39	2.96	0.77	700	3.11	1.04
50.0	25	4.32	24.5	0.83	1692	29.4	0.59
	35	5.00	93.2	1.35	433	37.1	0.15
	45	5.11	61.6	0.59	888	102	0.01
	55	5.11	62.0	0.57	2275	76.3	0.05

respectively. From inspection of the position of the points of the linearized Avrami equation, the formation of one to three linearized regions, in relation to the temperature and the contact time, is strongly suggested. So, one to three independent values of n_i ($i = 1$–3) and $k_{Av(i)}$ ($i = 1$–3) should also be considered. The calculated n_i and $k_{av,i}$ constants are different from 25 to 55°C. In this manner, for this temperature range, the sorption kinetics of Cr(VI) seem to present both temperature and contact time dependence. The experimental and calculated comparative values of the sorption amounts (q_t) in relation to the pseudo-first- and second-order and Avrami kinetics models are shown in Tables II and III. To evaluate the exponential kinetic model, chi-square (χ^2) tests were also done according to eq. (5). The kinetic parameters, presented in Table III, have excellent agreements of the experimental and calculated data were found using the Avrami model for all kinetic isotherms evaluated (χ^2 less than 3.38×10^{-6}).

In many experimental sorption systems the effect of transport in the solution is eliminated by rapid mechanical mixing, thus, it is not assumed to be involved in controlling of the overall sorption rate and can be ignored, as a rule.[9] To determine the contribution of the remaining steps, numerous kinetic models have been compared to predict the behavior of the experimental data. The most widely used are those assuming that step (iv) makes a significant contribution in the kinetics of a process. Here, this step is referred to as "surface reaction". The "surface reaction" term may not necessarily mean the actual chemical reaction occurring on the adsorbent surface involving the formation of chemical bonds. Interactions of physical nature (van der Waals forces, for instance) may also play a role. The crucial assumption behind this model is that the rate of the transfer of solute molecules from the solution (located in the direct vicinity of the surface) to the adsorbed phase either governs the overall rate of sorption process or at least is partially involved in it.[45]

The mechanistic interpretation of the Avrami constants, $k_{Av,i}$ and n_i, is difficult and open to interpretation.[46] Originally, n_i was held to have values between 1.0 and 4.0. In general, the values of n_i from 0.5 to about 1.3 have been related to surface reactions and from 3.0 to about 4.0 to three-dimensional interactions at solid/solution interfaces. When sorption occurs on specific sites, interactions may be random leading to high values for n (2, 3 or higher). In last stages of sorption, the sorption may be restricted to one or two dimensions. So, sorption saturation may lead to n_i values of 1, 2 or 3 for surface, edge and point sites in internal sites of the adsorbent, respectively.

The use of most kinetic models is usually been associated with the surface-reaction kinetic step as controlling the sorption rate.[47,48] However, this frequently is not the case. So, an intraparticle diffusion model was also used here to check Cr(VI) diffusion into GA-scale, using eq. (12):[47]

$$q_t = k_{\text{dif}} t^{1/2} + I \tag{12}$$

where k_{dif} is the intraparticle diffusion rate constant and I is the intercept.

The parameters of the Intraparticle diffusion kinetic model are presented in Table IV. If the intraparticle diffusion is involved in the sorption process, then a plot of $t^{1/2}$ *vs* q_t would result in a linear relationship and the particle diffusion would be the controlling step if this line passed through the origin.[47] When the plots do not pass through the origin, this is indicative of some degree of boundary layer control and this further show that the intraparticle diffusion is not the only rate-controlling step, but also other processes may control the rate of sorption,

TABLE III
Kinetic Parameters of the Avrami Kinetic Model for Sorption of Cr(VI) on Crosslinked Fibrillar Collagen on Corvina Scales

$C_i/10^{-4}$ (mol L^{-1})	Temperature (°C)	Avrami Kinetic Parameters						
		n_1	n_2	n_3	$k_{Av,1}/10^{-4}min^{-1}$	$k_{Av,2}/10^{-4}$ min^{-1}	$k_{Av,3}/10^{-4}min^{-1}$	$\chi^2/10^{-8}$
0.05	25	0.22	1.10	2.93	7.76	97.7	56.7	0.36
	35	1.07	1.50		87.8	67.1		0.13
	45	0.58	1.86	2.47	15.0	58.1	49.4	14.3
	55	1.04	1.45	2.76	31.9	47.4	37.5	1.16
0.50	25	0.41	1.25	1.85	66.4	58.1	37.5	33.7
	35	0.65	0.92	0.32	150	143	1288	25.2
	45	0.54	0.45	2.01	58.3	60.3	48.4	30.1
	55	0.85	1.32	2.14	39.5	42.2	39.6	74.6
5.00	25	0.36	0.97	1.48	68.9	77.2	64.3	28.4
	35	0.47	0.99	1.90	14.3	47.2	39.8	75
	45	0.58	1.44	3.86	6.65	32.7	33.7	105
	55	0.39	1.04	2.28	8.28	40.1	38.4	338

Standard deviation for n_i and $k_{Av,i}$ less than 5.0%.

all of which may be operating simultaneously. The values of the intercepts give an idea about the boundary layer thickness: the larger the intercept, the greater is the boundary layer effect.

Sorption kinetics is usually controlled by different mechanisms, including initial curved portions, attributed to rapid external diffusion or boundary layer diffusion and surface sorption, and gradual sorption stages due to intraparticle diffusion, followed by a final equilibrium plateau where the intraparticle diffusion starts to decrease due to the low concentration in solution as well as fewer available sorption sites. The values of the diffusion constants (k_{dif}) increase with temperature and the initial Cr(VI) concentration in solution. The boundary layer resistance is affected by the rate of sorption and increase in contact time, which reduce the resistance and increases the mobility of the adsorbate during sorption. However, the very low values of the intercepts (I) values showed in Table IV suggest that the Cr(VI) sorption boundary layer effects close to minimum values. So, the low values of both interaction enthalpies for water swelling and the boundary layer parameter of the intraparticle diffusion model indicate that internal diffusion of both water and Cr(VI) is a key step in sorption of Cr(VI) on GA-scale.

Because of the hydrophilic nature of their monomeric units, collageneous materials possess a remarkably high swelling capacity in water and, consequently, their networks are sufficiently expanded to allow a fast diffusion process for the studied adsorbates. Thus, the interaction between the adsorbate molecules and the most favorable sites within the polymeric structure will be facilitated for the expanded networks. These materials also have diffusion properties and possess an amphiphilic character. It is precisely this character of these sorbents what makes them so appealing, since water they are hydrophilic enough to swell considerably in water allowing fast diffusion processes for specific adsorbates, while at the same time they possess highly hydrophobic sites which trap adsorbate molecules or ions efficiently. It was also observed that the modeling of intraparticle diffusion seems to indicate a contribution of film diffusion on the control of sorption kinetics; however intraparticle diffusion was not the dominating mechanism (the multilinearity in the kinetic experiments indicated that two or more steps occur in the sorption processes).

The control of sorption performances of an adsorbent depends on the following physico-chemical factors: first, the nature of the adsorbent, such as its physical structure (porosity, particle size), its chemical structure (ionic charge), and functional groups (variety, density); second, the chemistry and accessibility of the adsorbate (e.g. its polarity, molecular weight and size); finally, the solution conditions,

TABLE IV
Intraparticle Diffusion Kinetic Parameters for Sorption of Cr(VI) on Crosslinked Fibrillar Collagen on Corvina Scales

T (°C)	$C_i/10^{-3}$ (mol L^{-1})	$k_{dif}/10^{-6}$ (mol $g^{-1}min^{-1}$)	$I/10^{-6}$ (mol g^{-1})
25	0.05	0.03	0.14
35		0.03	0.11
45		0.06	0.05
55		0.10	0.03
25	0.50	2.50	0.70
35		1.29	0.30
45		1.28	0.11
55		1.45	0.09
25	5.00	5.45	0.46
35		9.00	0.82
45		35.0	0.24
55		45.0	0.26

Average standard deviation of the results (%) = 5.0–5.9.

referring to its pH, temperature and the adsorbate concentration. So, the sorption mechanism is complex, probably simultaneously dominated by surface adsorption and diffusion into the collagen network, and chemisorption due to the presence of the specific chelating groups of collagen (mainly amides and amines) and ion-exchange interactions due to the presence of carboxylic groups of the amides of collagen structure. To confirm more details of sorption mechanisms of fish scales, more experiments will be carried out using other metals as adsorbates.

The maximum sorption capacity observed for Cr(VI) on GA-scale (39 mg g^{-1}) is comparable with literature reports, especially in relation to some commercial activated carbon samples.[49–55] Because of scarcity of consistent cost information in the literature data, cost comparisons are difficult to make. However, the relative cost of the material used in this study is supposed much lower than that of commercial activated carbons.

CONCLUSIONS

In this work, fibrillar collagen on Corvina fish scales were crosslinked with (poly)glutaraldehyde and used as a new material for sorption of Cr(VI) from aqueous solutions. Characterization has suggested that the crosslinked collagen of Corvina scale has higher denaturation temperature in relation to the raw scales. The water swelling interactions at crosslinked fibrillar collagen/water interfaces are slightly exothermic and interaction energies decreased with increasing temperature. FTIR spectra have suggested that electrostatic interactions between Corvina scales positive charges and chromate negative charges seem to constitute the majority of the interactions.

Sorption of Cr(VI) on GA-scale increase with the increasing of initial Cr(VI) concentration and decreases with temperature increasing. The kinetic data of Cr(VI) sorption on the scales were best fitted by the multilinear Avrami model. It was found that internal diffusion of both water and Cr(VI) is a key step in sorption of Cr(VI) on GA-scale. To confirm this mechanism, more experiments will be carried out using other metals as adsorbates.

The sorption capacity observed for Cr(VI) on GA-scale is found to be comparable with literature reports, especially in relation to some commercial activated carbon samples. So, GA-crosslinked fish scale has shown features of a new and promising adsorbent for sorption of Cr(VI) from aqueous solutions.

References

1. Srividya, K.; Mohanty, K. Chem Eng J 2009, 155, 666.
2. Tanriseven, A.; Zehra, O. Biochem Eng J 2008, 39, 430.
3. Sardohan, T.; Kir, E.; Gulec, A.; Cengeloglu, Y. Sep Purif Technol 2010, 74, 14.
4. Zhang, J. J.; Duan, R.; Ye, C.; Konno, K. J Food Biochem 2010, 34, 1343.
5. Stepnowski, P.; Ólafsson, G.; Helgason, H.; Jastorff, B. Aquaculture 2004, 232, 293.
6. World Health Organization. Guidelines for drinking-water quality, 3rd ed., Recommendations; World Health Organization: Geneva, 2004; Vol.1, pp 334–335.
7. Owlad, M.; Aroua, M. K.; Daud, W. A. W.; Baroutian, S. Water Air Soil Pollut 2009, 200, 59.
8. Akpor, O. B.; Muchie, M. Int J Phys Sci 2010, 5, 1807.
9. Saha, B.; Orvig, C. Coord Chem Rev 2010, 254, 2959.
10. Cestari, A. R.; Vieira, E. F. S.; Silva, R. C.; Andrade, M. A. S., Jr. J Colloid Interf Sci 2010, 352, 491.
11. Pagano, B.; Mattia, C. A.; Giancola, C. Int J Mol Sci 2009, 10, 2935.
12. McFarlane, N. A.; Wagner, N. J. Langmuir 2010, 26, 6262.
13. Dizge, N.; Keskinler, B.; Tanriseven, A. Colloids Surf B 2008, 66, 34.
14. Rivera-Utrilla, J.; Bautista-Toledo, I.; Ferro-Garcya, M. A.; Moreno-Castilla, C. J Chem Technol Biotechnol 2001, 76 1209.
15. Vieira, E. F. S.; Cestari, A. R.; Silva, R. G.; Pinto, A. A., Miranda, C. R.; Conceição, A. C. F. Thermochim Acta 2004, 419, 45.
16. Vieira, E. F. S.; da Costa, L. P.; Cestari, A. R. J Appl Polym Sci 2010, 118, 857.
17. Figueiredo, H.; Silva, B.; Quintelas, C.; Neves, I. C.; Tavares, T. Chem Eng J 2010, 163, 22.
18. Cestari, A. R.; Vieira, E. F. S.; Matos, J. D. S.; dos Anjos, D. S. C. J Colloid Interf Sci 2005, 285, 288.
19. Bigi, A.; Burghammer, M.; Falconi, R.; Koch, M. H. J.; Panzavolta, S.; Riekel, C. J Struct Biol 2001, 136, 137.
20. Migneault, I.; Dartiguenave, C.; Bertrand, M. J.; Waldron, K. C. Biotechniques 2004, 37, 790.
21. Guisán, J. M. Enzyme Microb Technol 1988, 10, 375.
22. Liu, W. T.; Zhang, Y.; LI, G. Y.; Miao, Y. Q.; Wu, X. H. J Fish Biol 2008, 72 1055.
23. Kotas, J.; Stasicka, Z. Environ Pollut 2000, 107, 263.
24. Rivas, B. L.; Peric, I. M.; Villegas, S. Polym Bull 2010, 65, 917.
25. Mack, C.; Wilhelm, B.; Duncan, J. R.; Burgess, J. E. Biotechnol Adv 2007, 25 264.
26. Pati, F.; Adhikari, B.; Dhara, S. Bioresour Technol 2010, 101, 3737.
27. Nadeem, R.; Ansari, T. M.; Khalid, A. M. J Hazard Mater 2008, 156, 64.
28. Kumar, R.; Sripriya, R.; Balaji, S. M.; Kumar, M. S.; Sehgal, P. K. J Mol Struct 2011, 994, 117.
29. Gu, Y. W.; Tay, B. Y.; Lim, C. S.; Yong, M. S. Biomaterials 2005, 26, 6916.
30. Bigi, A.; Cojazzi, G.; Panzavolta, S.; Rubini, K.; Roveri, N. Biomaterials 2001, 22, 763.
31. Ikoma, T.; Kobayashi, H.; Tanaka, J.; Walsh, D.; Mann, S. J. Struct Biol 2003, 142, 327.
32. Villanueva-Espinosa, J. F.; Hernández-Esparza, M.; Ruiz Treviso, F. A. Ind Eng Chem Res 2001, 40, 3563.
33. Agarwal, G. S.; Bhuptawat, H. K.; Chaudhari, S. Bioresour Technol 2006, 97 949.
34. Zahn, D.; Hochrein, O. Phys Chem B 2003, 5, 4004.
35. Wadso, I. Chem Soc Rev 1997, 26, 79.
36. Chowdhry, B. Z.; Beezer, A. E.; Greenhow, E. J. Talanta 1983, 30, 209.
37. Berling, D.; Jonsson, B.; Olofsson, G. J. Solution Chem 1999, 28, 693.
38. Tarasevich, Y. I. Colloid J 2007, 69, 212.
39. Lopes, E. C. N.; dos Anjos, F. S. C.; Vieira, E. F. S.; Cestari, A. R. J. Colloid Interf Sci 2003, 263, 542.
40. Plazinski, W.; Rudzinski, W.; Plazinska, A. Adv Colloid Interface Sci 2009, 152, 2.
41. El-Khaiary, M. I.; Gihan F. M. Hydrometallurgy 2011, 105, 314–320.

42. Cotoruelo, L. M.; Marques, M. D.; Rodríguez-Mirasol, J.; Cordero, T.; Rodríguez, J. J Ind Eng Chem Res 2007, 46, 2853.
43. Babu, S. S. Int Mater Rev 2009, 54, 333.
44. Qiu, H.; Lv, L.; Bing-cai, P.; Zhanag, Q-J.; Zhang, W-M.; Zhang, Q-X. J Zhejiang Univ Sci A 2009, 10, 716.
45. Ho, Y-S. Process Biochem. 1999, 34, 451.
46. Yang, X.; Al-Duri, B. J Colloid Interf Sci 2005, 287, 25.
47. Avranas, A.; Papadopoulos, N.; Papoutsi, D.; Sotiropoulos, S. Langmuir 2000, 16, 6043.
48. Ocampo-Perez, R.; Levya-Ramos, R.; Alonso-Davila, P.; Rivera-Utrilla, J.; Sanchez-Polo, M. Chem Eng J 2010, 165, 133.
49. Selomulya, C.; Meeyoo, V.; Amal, R. J Chem Technol Biotechnol 1999, 74, 111.
50. Hu, Z.; Lei, L.; Li, Y.; Ni, Y. Sep Purif Technol 2003, 31, 13.
51. Dakiky, M.; Khamis, M.; Manassra, A.; Mereb, M. Adv Environ Res 2002, 6, 533.
52. Zhao, N.; Na, W.; Li, J.; Qiao, Z.; Jing, C.; Fei, H. Chem Eng J 2005, 115, 133.
53. Argun, M. E.; Dursun, S.; Ozdemir, C.; Karatas, M. J Hazard Mater 2007, 141, 77.
54. Schmuhl, R.; Krieg, H. M.; Keizer, K. Water SA 2001, 27, 1.
55. Hamadi, N. K., Chen, X. D.; Farid, M. M.; Lu, M. G. Q. Chem Eng J 2001, 84, 95.